Preprints of the 19th World Congress
The International Federation of Automatic Control
Cape Town, South Africa. August 24-29, 2014

A robust fractional order controller for an EAF electrode position system

Feliu-Batlle V.*, Rivas-Perez R., Castillo-Garcia F.J.*, Rodriguez-Martinez C.A.****

*** Escuela Técnica Superior de Ingenieros Industriales, Universidad de Castilla-La Mancha, Campus Universitario s/n, Ciudad Real, C.P. 13005, Spain (e-mail: vicente.feliu@uclm.es; fernando.castillo@uclm.es)*
*** Department of Automatica and Computer Science, Havana Polytechnic University, Calle 114 No 11901, CUJAE, Marianao, Habana, C.P. 19390, Cuba (e-mail: rivas@electrica.cujae.edu.cu; cmartinez@electrica.cujae.edu.cu)*

Abstract: This paper proposes a simple fractional-order controller with a PI^{α} structure for controlling the position of the electrodes of an electric arc furnace (EAF)**.** The dynamics of one of the three electrodes of an industrial EAF process was experimentally identified. Models of the electrode position system and the furnace electrical system (electric arc impedance model) were obtained. This identification procedure yielded an equivalent fourth order plus time delay transfer function, and showed strong plant parameter variations and measured and unmeasured disturbances**.** We therefore propose a new methodology for the design of fractional-order robust controllers for this system. By carrying out a partial inversion of the dynamics, a method for fractional-order robust control of first order plus time delay plants was developed and applied to this process. It was shown that the attained controllers significantly outperformed the robustness achieved with *PI* and *PID* controller (also combined with the partial dynamics inversion term), while adding only moderate complexity to the control structure.

Keywords: robust control systems; fractional order controllers; electric arc furnace; electrode position system.

1. INTRODUCTION

Metallurgic industry pursues increasing energy efficiency of its production processes because the effective and sustainable use of energy is becoming more important in the world owing to the energetic crisis and to environmental pollution. Electric arc furnaces (EAF) are widely used in this industry for melting scrap or other metals (Mullinger and Jenkins, 2008) because electric arcs allow to obtain high temperatures necessary to melt or/and to realize some chemical reactions. EAF are considered as one of the most energy consumption plants. A significant amount of energy is being lost in most of the EAF because of inaccurate control (Li and Mao, 2012).
Three graphite electrodes are commonly used, which are connected to the electrical supply by a three-phase power transformer. These electrodes are very heavy (up to tenth tons). The circuit closes through the metal mass that will be molten. The electric arc appears when the electrodes are near the metal mass. Usually, the distance between the electrode and the metal mass is 5-15 cm. Typical electric power levels for EAF range from 10 MW to 100 MW. The electric power depends on the length of the arc which is controlled by means of an electrode position controller (Balan et al., 2007). Two variables can be used in the electrode position feedback control: the arc-impedance or the arc-current. Any deviation from the optimum arc length impairs the power utilization efficiency. Then the electrode position controller plays an important role, by which a reference arc-impedance or arc-current is maintained to guarantee steady power input to the scrap in the EAF. Fig. 1 shows a diagram of an EAF.
The scrap surface is irregular and, as it is partially melt, it moves, changing its contour. Thus, random unmeasured disturbances in the arc length occur continuously (Balan et al., 2007). The electrode position controller must reject such disturbances by moving the electrode to maintain the arc length at its preset value. Moreover, the electrode mass changes constantly because it is consumed during the melting process, originating large variations in the dynamic parameters of the electrode position system (Li and Mao, 2012).

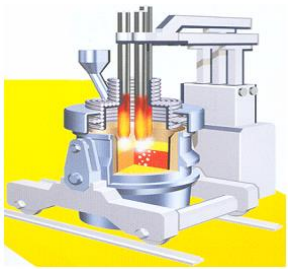

Fig. 1. Schematic diagram of an EAF.

A fast time response with small overshoot is necessary for the electrode position control system in order to optimize the power utilization efficiency (Morris and Sterling, 1975). However, these requirements are difficult to fulfill since the electrode position system dynamics shows high nonlinearity, strong coupling among the phases, time delay, time-varying dynamic parameters, and diverse disturbances (Li, and Mao, 2012). Then a robust controller for the electrode position system of an EAF is advisable because it reduces the energy consumption and environmental pollution, while increases efficiency and safety of the furnace (Balan et al., 2007).
At present, this system is mostly controlled by *PID* controllers (Guan et al., 2009). But some studies showed that they are inadequate for plants that have complex dynamic

behaviors. Consequently, often these controllers increase power consumption and reduce the efficiency of the furnace.
Billings and Nicholson (1977) proposed a temperature weighing adaptive controller, which uses ambient arc-temperature as an additional control parameter to weight the error feedback. However, this controller is difficult to implement because measuring temperature in an EAF is a difficult task. Other controllers use a linear model of the process (e.g. Bekker et al, 2000). However, they are only effective around the operating points and have several limitations in practical applications in which the process dynamic parameters largely change. Intelligent controllers have also been suggested. Staib and Bliss (1995) proposed a neural network to control the electrode position, which can learn online during the smell process. Zhang (2006) presented an adaptive inverse control system based on radial basis functions neural network, which identified and decoupled the process in real time. However, this system requires a high-speed acquisition and processing device for implementing the control system. Guan et al. (2009) proposed an adaptive fuzzy sliding mode controller for an electrode regulator system, which behaved robust to some process uncertainties and disturbances, but the stability of the control system was not guaranteed. A robust adaptive neural network controller was derived by Li and Mao (2012), but the practical implementation of this controller was complicated. It should be mentioned that the controller to be used must be simple enough to allow its real time implementation, while it must be robust to plant dynamic parameter variations and disturbances.
Besides, fractional operators have recently shown satisfactory results when applied to modelling and controlling processes with complex dynamics. Performance and robustness of *PID* controllers can be improved by means of their generalization to $PI^{\alpha}D^{\lambda}$ fractional controllers (Podlubny, 1999). Several recent works proposed the application of fractional order controllers to industrial furnaces (e.g. Duarte Isfer et al., 2010; Rodriguez-Martinez et al., 2011; Feliu-Batlle et al., 2013). They describe the different behaviors that can be achieved in the controlled systems by changing the fractional order of the differential/integral operators, but no tuning methodology or robustness analysis was provided in them.
This article develops a new methodology for designing fractional order controllers for the electrode position system of an EAF, robust to plant parameter variations. In this paper, all the modelling and control methodologies have been carried out for a real industrial EAF, whose nominal dynamics and ranges of parameter variations have been experimentally determined. The performance of the proposed controller has been tested by running simulations using the transfer functions obtained from the real plant.
This paper is organized as follows. Section 2 describes the electric arc furnace under study and develops a linear model of the electrode position system, which considers the ranges of dynamic parameter variations. Section 3 states the robust control objectives. Section 4 presents three control schemes to be studied and compared. Section 5 describes the control design procedure and conclusions are drawn in Section 6.

2. SYSTEM DESCRIPTION AND DYNAMIC MODEL

2.1. EAF description

We study the EAF of Antillana de Acero steel company in Havana, Cuba. This is a 3-phase AC furnace with a 110 tons production. The electric power consumption is about 410 kWh/ton. The electrode system of this furnace has three main subsystems: the power supply, the hydraulic electrode position and the electric arc.
The power supply system includes a high voltage transmission circuit and an arc furnace transformer. The hydraulic electrode position system includes an hydraulic tank, hydraulic pumps, hydraulic cylinders, a secondary hydraulic supply and the control valves. Each electrode is positioned individually by its own controller, which operates a control valve that adjusts the flow from the hydraulic tank to the hydraulic cylinder and produces a vertical movement. This subsystem is an important part of the furnace operation, since the position of the electrode directly influences the arcs length and, consequently, their impedances. Thus this subsystem controls the power and the resistance (through the length) of each arc according to the operation conditions. It is important to point out that arc-impedance control that is based on maintaining the resistance of the arcs at a constant value yields, in general, a non-interacting control of the three electrodes position controllers'. A disturbance in one phase alters all the currents and voltages, but only the impedance of the disturbed phase changes. Arc-impedance control can therefore be considered as composed of three independent electrode position controllers. Conversely current control, which controls the magnitude of the phase currents, produces an inherent interaction between the three electrode position controllers (Billings and Nicholson, 1977). The scheme of the electrode position system using arc-impedance control (per one phase) is shown in Fig. 2.

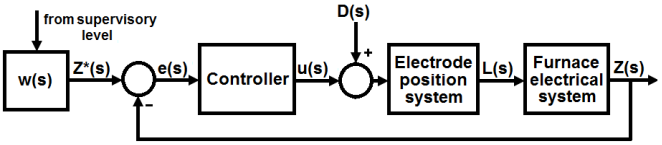

Fig. 2. Scheme of the electrode position control system.

2.2. Dynamic mathematical model

Several mathematical models have been proposed for EAF (see e.g. Billings et al., 1979; Balan et al., 2007). However, these models are usually too complex to be applied in control design. Simpler dynamic models suitable for control design can be obtained using system identification methods (see e.g. Billings et al., 1979; Rodriguez-Martinez et al., 2011). We consider the arc-impedance Z(t) of the electrode as the controlled variable and the electrode position L(t) as the manipulated variable. Z(t) is calculated by the PLC that controls the furnace as the quotient of phase voltage and phase current, which are easily measured. The identification of a single electrode was carried out. Variables Z(t) and L(t) were measured in closed loop control operation using a computer (PC) with a data acquisition card of 1 second sampling time. Disturbances are the large conductance changes and can be modeled as a stepwise disturbance D(t) applied to the input variable of the process u(t), as it is shown in Fig. 2.
Initially, step input tests on the control valve of the electrode position system (in mV) were analyzed to verify the linearity

of the system over the operating range and to know the appropriate values of the time delay, process model order, effect of disturbances, etc. Then, a pseudo-random binary sequence (PRBS) was applied. Data obtained of the position system and impedance of electrode 1 is shown in Fig. 3.

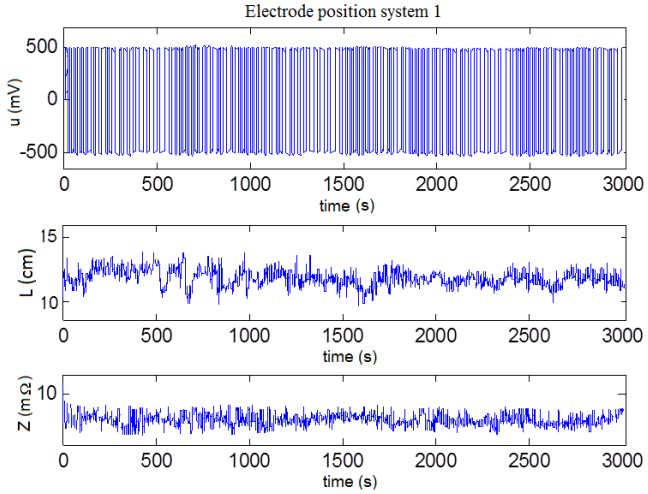

Fig. 3. Experimental data obtained in the electrode position system 1 using a PRBS.

A direct system identification procedure (Garnier and Wang, 2008) was applied to the recorded data. It yielded the following nominal models of the position system of electrode 1 and the furnace electrical system 1, respectively:

$$G_{eps}(s) = \frac{K_0}{s\cdot(T_0\cdot s+1)}e^{-\tau_0\cdot s} = \frac{2.2}{s\cdot(1.55\,s+1)}e^{-2s}; \quad (1)$$

$$G_{fes}(s) = \frac{0.65}{(1.7s+1)(0.9s+1)}. \quad (2)$$

Developing more real-time experiments in the electrode position system of our EAF, and using a robust system identification procedure, it was shown that variations of the electrode mass in the operation range together with the movements of the electrodes and the scrap originate variations in the dynamic parameters of the mathematical model (1) in the ranges $[K_{\min}, K_{\max}]$, $[T_{\min}, T_{\max}]$, $[\tau_{\min}, \tau_{\max}]$:

$$1.1 \le K(t) \le 5.5;\quad 0.7 \le T(t) \le 3.9;\ 1 \le \tau(t) \le 4. \quad (3)$$

Any controller designed for the effective control of the electrode position system should therefore guarantee a minimum level of performance in the whole range of variation of the dynamic parameters of the mathematical model (1)-(3).

3. CONTROL OBJECTIVES

Taking into account the previous considerations, we propose as control objectives: 1) a small overshoot in the nominal process response, 2) a response as fast as possible of the nominal process, and 3) a guaranteed minimum level of performance in all the range of variation of process parameters.

Desired overshoot (M_p) and settling time (t_s) of the closed loop system can be approximately achieved by designing two frequency specifications (e.g. Ogata, 1993): phase margin (ϕ_m), and gain crossover frequency (ω_c). If a second order system were used as reference, the following approximate relations would hold:

a) Phase margin versus damping ratio with an error lower than 1^o: $\phi_m \approx -55.78\cdot\zeta^2 + 133.58\cdot\zeta - 0.9$. We also use the well known formula $\zeta = 1/\sqrt{1+(\pi/\log(M_p))^2}$. These systems must be operated with very small overshoot (Morris and Sterling, 1975). Then a design value $M_{p0} = 2\%$ is chosen for the nominal process, and the two previous expresions yield values $\zeta_0 = 0.8$ and $\phi_{m0} \approx 70^o$.

b) The closed loop settling time versus the gain crossover frequency: $t_s \approx \pi/\omega_c$. The open loop settling time of the nominal overall system (1), (2) is $10.8\,s$. We choose a closed loop settling time 50% larger than this value in order to achieve robustness in some neighbourhood of the nominal process. Then the desired settling time for our nominal system is $t_{s0} = 16.2$ s, which yields, using the previous formula, a value $\omega_{c0} = \pi/t_{s0} = 0.194$ rad / s.

c) The robustness specification, expressed as a minimum performance to be accomplished in all the parameters range (3), is defined by a minimum phase margin ($\bar{\phi}_m$) and a minimum gain crossover frequency ($\bar{\omega}_c$), to be verified simultaneously:

$$\phi_m \ge \bar{\phi}_m,\quad \omega_c \ge \bar{\omega}_c,\quad \forall K, T, \tau \quad (4)$$

Fulfilment of these frequency specifications will not guarantee exact verification of time specifications because our process is quite different of a second order system. However, they allow designing closed loop systems which yield responses that reasonably approximate these time specifications, and moreover guarantee a robust behaviour in (3) (frequency specifications are generally better suited to design robustness features than time specifications).

In order to assess the level of robustness achieved by a controller, a methodology based in the design technique developed in Castillo et al. (2013) is used. It consists of: 1) calculating the robustness region of each controller, 2) defining a scalar index representative of such region and 3) comparing controller's robustness by comparing the associated indexes.

First note that changes in the time delay do not modify the gain crossover frequency of the system. However, increasing the time delay reduces the phase margin. Then given a pair (K,T), the worst case in order to fulfil (4) happens when the time delay value is maximum (τ=τ_{max}). Then the robustness analysis will be carried out considering this worst case: τ is set to τ_{max} and volumes defined by variations in (K,T,τ) are reduced to areas (K,T). Subsequently, we define the robustness index ρ of a controller as the maximum value such that all the points of the area given by the inequality

$$\max\left(\frac{K-K_0}{K_{\min}-K_0}, \frac{K-K_0}{K_{\max}-K_0}, \frac{T-T_0}{T_{\min}-T_0}, \frac{T-T_0}{T_{\max}-T_0}\right) \le \rho, \quad (5)$$

verify condition (4). Regions defined by (5) are the rectangles shown in Fig. 4. These shapes have been chosen in order to

be consistent with the parameter variation region defined by (3). The largest rectangle among the ones shown in this figure describes the parametric variations in (*K*,*T*) given by (3), which corresponds to ρ=1.

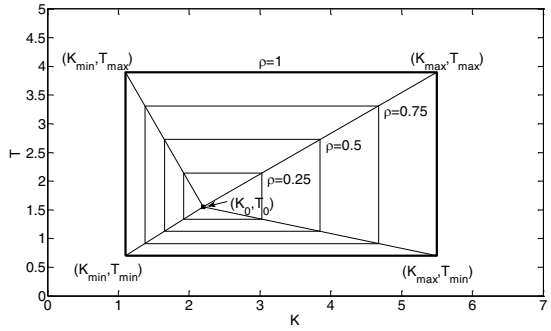

Fig. 4. Representation of the areas associated to the robustness index ρ: rectangles around (K_0, T_0).

4. CONTROL SCHEMES

Our control approach is based on: 1) cancelling the well determined subsystem of the plant by dynamic inversion, and 2) designing a fractional order *PI* controller (*FPI*):

$$R(s) = K_p + \frac{K_i}{s^\alpha}, \quad 0 < \alpha < 2 \cdot \tag{6}$$

This control scheme is shown in Fig. 5a, in which the dynamic inversion is performed by

$$C(s) = \frac{s \cdot G_{fes}^{-1}(s)}{(1+\mu \cdot s)^3} = 1.5385 \ \frac{s \cdot (1+0.9s) \cdot (1+1.7s)}{(1+\mu \cdot s)^3}, \tag{7}$$

where μ is chosen such that $\mu^{-1} >> 10 \cdot \omega_{c0}$ in order to make $C(s)$ proper without modifying the desired closed loop dynamics. Assuming $\mu \approx 0$, the remaining open loop dynamics is

$$P(s) = G_{eps}(s) \cdot G_{fes}(s) \cdot C(s) = K \cdot e^{-\tau \cdot s} / (1 + T \cdot s), \tag{8}$$

and the closed loop transfer function is

$$M(s) = \frac{K \cdot (K_p s^\alpha + K_i) \cdot e^{-\tau \cdot s}}{s^\alpha \cdot (1+Ts) + K \cdot (K_p s^\alpha + K_i) \cdot e^{-\tau \cdot s}}. \tag{9}$$

This controller has the drawback of producing a large overshoot in the step response, which is caused by the factor $K_p s^\alpha + K_i$ that appears in the numerator of (9).

An improvement of this scheme is the one shown in Fig. 5b, which has the closed loop transfer function

$$M(s) = \frac{K \cdot K_i \cdot e^{-\tau \cdot s}}{s^\alpha \cdot (1+Ts) + K \cdot (K_p s^\alpha + K_i) \cdot e^{-\tau \cdot s}}. \tag{10}$$

The characteristic equations of (9) and (10) coincide but, in the last case, the factor of the numerator has been removed. Then the time response to a step command is smoother but the settling time is larger than in (9) because fractional order dynamics at low frequencies dominate in the long term.

Then a third scheme is proposed, shown in Fig. 5c, which combines (10) with a prefilter $F(s)$ that speeds up the response of the system to a step command. This prefilter cancels the dominant poles of M(s) and is designed as follows. Taking into account that the low frequencies of interest verify that $\tau \cdot \omega < 0.5$, then $e^{-\tau \cdot s} \approx (1 - 0.5 \cdot \tau \cdot s)/(1 + 0.5 \cdot \tau \cdot s)$ and, substituting this in (10) for the nominal plant, yields

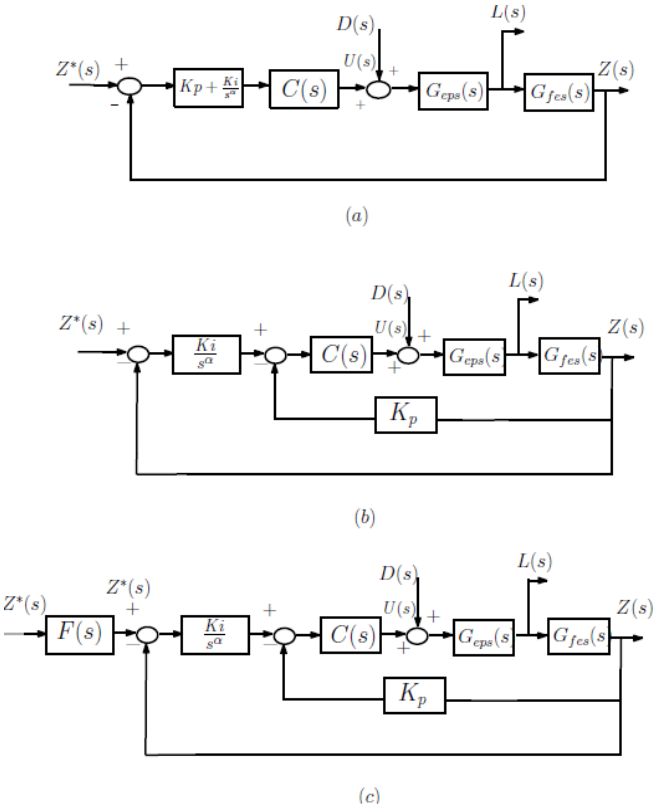

Fig. 5. Control schemes.

$$M_0(s) \approx \frac{K_0 \cdot K_i \cdot (1 - \frac{\tau_0}{2} s)}{s^\alpha \cdot (1+T_0 s) \cdot (1+\frac{\tau_0}{2} s) + K_0 \cdot (K_p s^\alpha + K_i) \cdot (1 - \frac{\tau_0}{2} s)}. \tag{11}$$

The low frequency response of $M_0(s)$ is obtained by neglecting the higher order terms of its denominator:

$$M_0^{lowf}(s) \approx \frac{K_0 \cdot K_i \cdot (1 - 0.5 \cdot \tau_0 \cdot s)}{K_0 \cdot K_i + (1 + K_0 \cdot K_p) s^\alpha - K_0 \cdot K_i \cdot 0.5 \cdot \tau_0 \cdot s}, \tag{12}$$

and the filter proposed to cancel these dynamics is

$$F(s) = \frac{1 + (1 + (K_0 \cdot K_i)^{-1}) s^\alpha - 0.5 \cdot \tau_0 \cdot s}{(1 + \lambda \cdot s)^3}, \tag{13}$$

where λ is chosen such that a smooth response is obtained. Controllers of Figs. 5a, b and c yield the same closed loop characteristic equation. Then all of them will exhibit the same robustness features.

5. CONTROLLER DESIGN

Controllers (6) have three parameters to be designed while we have only two frequency specifications (ϕ_{m0}, ω_{c0}). They are designed for the remaining dynamics (8) of the nominal process. Provided that the fractional order α is known, these

controllers can be obtained from (e.g. Castillo et al, 2013):

$$K_i = \frac{\omega_{c0}^{\alpha}}{K_0 \cdot \sin\left(\frac{\pi}{2}\alpha\right)}\left[T_0 \cdot \omega_{c0} \cdot \cos(\gamma) + \sin(\gamma)\right];$$
$$K_p = \frac{-1}{K_0 \cdot \sin\left(\frac{\pi}{2}\alpha\right)}\left[T_0 \cdot \omega_{c0} \cdot \cos\left(\gamma + \frac{\pi}{2}\alpha\right) + \sin\left(\gamma + \frac{\pi}{2}\alpha\right)\right] \quad (14)$$

where $\gamma = \phi_{m0} + \tau_0 \cdot \omega_{c0}$.

We also consider *PID* controllers, which also have three parameters to be tuned. Provided that K_i is known, K_p and K_d can be obtained, such that specifications (ϕ_{m0}, ω_{c0}) are verified, from the expressions:

$$K_p = -\Re(\chi); \quad K_d = \frac{K_i - \omega_{c0} \cdot \Im(\chi)}{\omega_{c0}^2}, \quad (15)$$

where $\chi = e^{j\cdot\gamma} \cdot (1 + j \cdot T_0 \cdot \omega_{c0}) / K_0$, and $\Re()$ and $\Im()$ represent real and imaginary components of a complex number respectively. Simple closed loop stability conditions impose that $0 < K_i < \omega_{c0} \cdot \Im(\chi) + \omega_{c0}^2 \cdot T_0 / K_0$.

The robustness specifications are $\bar{\phi}_m = 0.6 \cdot \phi_{m0} = 42°$ and $\bar{\omega}_c = 0.5 \cdot \omega_{c0} = 0.097$ rad/s. Figs. 6a and 6.b show the robustness attained with the *FPI* and *PID* controllers, in function of α and K_i respectively. These figures show that robustness condition (4) is only attained in a small area of the parameter variation region (3): ρ=0.21 in the *FPI* and ρ=0.1 in the *PID*, while it is necessary to reach the value ρ=1 in order achieve robustness in all the region (3). Note that *PI* controllers are particular elements of these two families and are marked in Figs. 6a and b. Controllers that significantly outperform the *PI* robustness can be found in both families.

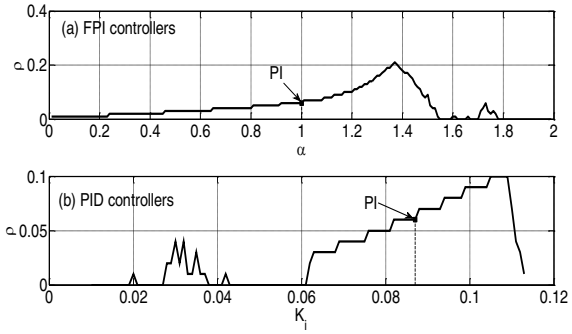

Fig. 6. Robustness index ρ with ω_{c0} = 0.194 rad/s.

Subsequently, the phase margins $\phi_{m0} \approx 70°$ and $\bar{\phi}_m = 42°$ are maintained, while gradually reducing the nominal gain crossover frequency ω_{c0}, and maintaining the ratio $\bar{\omega}_c = 0.5 \cdot \omega_{c0}$. Then the system response becomes slower but, in turn, the maximum value of ρ expands. This process is carried out until one of the elements of any of the families of controllers, either the *FPI* or the *PID*, reaches ρ = 1. This is achieved with a value $\omega_{c0} = 0.09$ rad/s, in which a ρ = 1.06 is reached by a *FPI* controller of α = 1.27:

$$R(s) = 0.1931 + \frac{0.0236}{s^{1.27}}. \quad (16)$$

Fig. 7 presents the robustness indexes obtained with the *FPI* and *PID* families for the specification ω_{c0} = 0.09 rad/s. It shows that: 1) the *FPI* family is much more robust than the *PID* family (maximum ρ attained with a *PID* is only 0.35), 2) controller (16) is much more robust than the *PI*, which has a ρ value of 0.3.

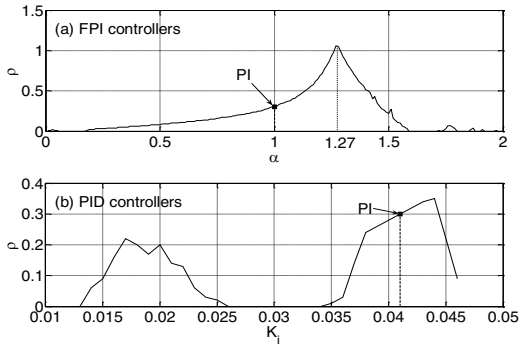

Fig. 7. Robustness index ρ with ω_{c0} = 0.09 rad/s.

The closed loop process has been simulated for the three control schemes of Fig. 5 using the cancellation term (7) with μ=0.05, which clearly verifies that $\mu^{-1} >> 10 \cdot \omega_{c0}$. Parameter λ of filter (13) has been set to 4.5. Fig. 8 shows the time responses *Z(t)* to step commands of the three control schemes in the case of the nominal plant. Fig. 9a shows the corresponding movements of the electrode *L(t)* and Fig. 9b the control signals *u(t)*. These responses show that the smoothest movements are achieved with scheme (c) which, besides, exhibits the smaller settling time.

Fig. 10 shows the responses attained with several extreme combinations of the process parameters. It illustrates that scheme (c) usually provides the most damped response with the smallest settling time. We mention that the robustness index ρ=1 can not be achieved by any *PID* controller (it includes the *PI* as a particular case), which even became unstable for some parameter combinations. For example, if ω_{c0} were reduced 10 times and set to 0.009 rad/s (a system ten times slower), the maximum ρ achieved with the *PID* family would be 0.67 - which corresponds to the *PI* controller – which is still far away from the desired value ρ=1. Finally, note that variables of Figs. 8, 9 and 10 are increments with respect to the equilibrium point and have been normalized for comparison purposes.

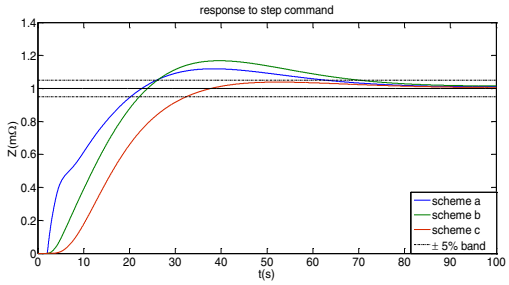

Fig. 8. Output responses to a step command of the schemes of Fig. 5.

6. CONCLUSIONS

The control of the electrode position system of an electric arc

furnace (EAF) robust to plant parameter variations has been studied, where the controlled variable was the arc-impedance. The dynamics of one electrode of an industrial furnace was experimentally identified, and the range of parameter variations was characterized.

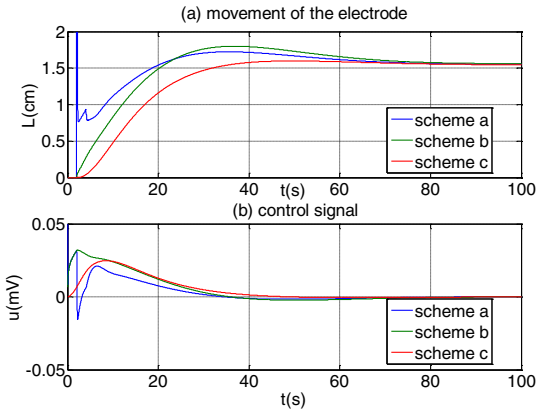

Fig. 9. Responses with control schemes of Fig.5: (a) electrode position movements L(t), (b) control signals u(t).

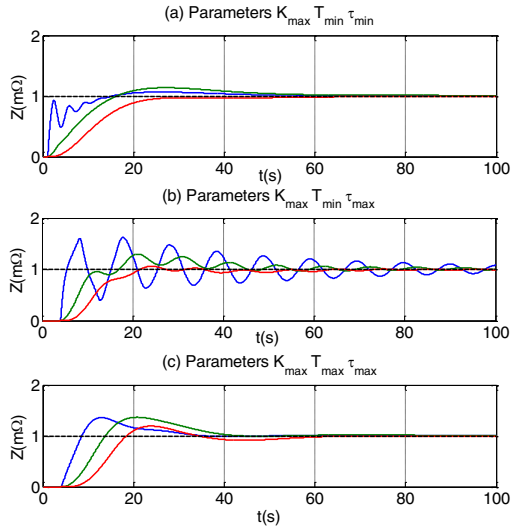

Fig. 10. Responses in the worst cases combinations of parameters: scheme (a) in blue, scheme (b) in green and scheme (c) in red.

A methodology has been proposed here in order to assess the robustness of different controllers. Nor *PI* or *PID* controllers could fulfill the robustness requirements. However, we showed that a simple modification of the *PI* controller, the fractional order *PI* controller (6), which has three parameters to be tuned like the *PID*, drastically improved the robustness of the previous controllers (about 200% improvement). It allowed to easily reaching the robustness specification at the price of a moderate reduction of the system response speed. Besides, robustness could not be achieved with a *PID*, even if the speed of the step response were drastically reduced.
Three implementation schemes of controller (6) were studied. We concluded that the third one, that included a fractional order prefilter, yielded the best results.

REFERENCES

Balan, R., Maties, V. Hancu, O., Stan S., and Ciprian L. (2007). Modeling and control of an electric arc furnace. In: *Proceedings of Mediterranean Conference on Control and Automation*, Athens, Greece.

Bekker, J.G., Craig I.K. and Pistorius P.C. (2000). Model predictive control of an electric arc furnace off-gas process. *Control Engineering Practice*, 8, 445–455.

Billings, S.A. and H., Nicholson (1977). Temperature weighting adaptive controller for electric arc furnaces. *Ironmaking and Steelmaking*, 4, 216-221.

Billings, S.A., Boland F.M., and Nicholson H. (1979). Electric arc furnace modelling and control. *Automatica*, 15, 137-148.

Castillo-García, F.J., Feliu-Batlle V. and Rivas-Perez, R (2013). Frequency specification regions of fractional-order PI controllers for first order plus time delay processes. *Journal of Process Control*, 23, 598-612.

Duarte Isfer, L.A., Kaminski Lenzi, E. Marcelo Teixeira, G. and Kaminski Lenzi, M. (2010). Fractional control of an industrial furnace. *Acta Scientiarum. Technology*, 32(3), 279-285.

Feliu-Batlle, V., Rivas-Perez, R. and Castillo-Garcia, F.J. (2013). Simple fractional order controller combined with a Smith predictor for temperature control in a steel slab reheating furnace. *International Journal of Control, Automation, and Systems*, 11(3), 533-544.

Garnier, H. and Wang, L. (2008). *Identification of continuous-time models from sampled data*. Springer-Verlag, London.

Guan, P., Li, J.C. and Liu, X.H. (2009). Direct adaptive fuzzy sliding mode control of arc furnace electrode regulator system. In: *Proceedings of Chine Control and Decision Conference*, Guilin, IEEE Press, 2776-2781, Chine.

Li, L. and Mao, Z.Z. (2012). A novel robust adaptive controller for EAF electrode regulator system based on approximate model method. *J. Cent. South Univ.,* 19, 2158-2166.

Morris, A.S. and Sterling, M.J.H. (1975). Analysis of electrode position controllers for electric arc steelmaking furnaces'. *Iron & Steel lnt.,* 48, 291-298.

Mullinger, P. and Jenkins, B. (2008). *Industrial and process furnaces. Principles, design and operation*. Elsevier, Oxford.

Ogata, K. (1993). *Modern Control Engineering*, Prentice Hall, Englewood Cliffs, New Jersey, USA.

Podlubny, I. (1999). *Fractional differential equations*. Academic Press, San Diego.

Rodriguez-Martinez, C.A., Rivas-Perez, R. Feliu-Batlle, V. and Castillo-Garcia, F. (2011). Fractional order control system of EAF of Antillana de Acero. In: *Proceedings of X International Symposium on Automation,* Informatica, La Habana, Cuba.

Staib, W.E. and Bliss, N.G. (1995). Neural network control system for the electric arc furnaces. *Metallurgical Plant and Technology International*, 18(2), 58-60.

Zhang, S.D. (2006). Decoupling control for electrode system in electric arc furnace based on neural network inverse identification. In: *Proceedings of Sixth International Conference on Intelligent Systems Design and Applications*, Ji´nan, IEEE Press, 112-116, Chine.